Journal of Applied Mechanics and Technical Physics, Vol. 50, No. 4, pp. 589–598, 2009

UNSTEADY BEHAVIOR OF AN ELASTIC ARTICULATED BEAM FLOATING ON SHALLOW WATER

I. V. Sturova

UDC 532.591+539.3

The unsteady behavior of an elastic beam composed of hinged homogeneous sections, which freely floats on the surface of an ideal incompressible fluid, is studied within the framework of the linear shallow water theory. The unsteady behavior of the beam is due to incidence of a localized surface wave or initial deformation. Beam deflection is sought in the form of an expansion with respect to eigenfunctions of oscillations in vacuum with time-dependent amplitudes. The problem is reduced to solving an infinite system of ordinary differential equations for unknown amplitudes. The beam behavior with different actions of the medium and hinge positions is studied.

Key words: *hydroelasticity, floating articulated plate, shallow water, unsteady response.*

The hydroelastic behavior of various bodies (ice fields, offshore platforms, and breakwaters) floating on the fluid surface is studied in solving applied problems. In the course of mathematical modeling, such bodies are often considered as thin elastic plates, because their horizontal sizes are much greater than their thickness. The major part of research of the behavior of floating bodies was performed under the assumption that the plate has homogeneous structural properties. In reality, however, both ice fields and artificial structures are not homogeneous. Structural heterogeneity can be caused by variation of the mass and rigidity coefficients along the plate and by the presence of hinged joints.

We confine ourselves to considering a very simple case of a plate composed of hinged homogeneous sections. For ice fields, such a situation is observed in the case of free overlapping of ice floes. In artificial structures, individual sections can be connected by simple hinged joints.

By the moment, the behavior of an articulated plate has been studied only for a linear problem of scattering of periodic surface waves under the assumption that the fluid flow and plate deformation are periodic functions of time. Oblique incidence of surface waves onto an elastic semi-infinite compound plate floating on the free surface of a finite-depth fluid was considered in [1]. In that study, the frontal section of a constant-width plate was connected by an elastic hinge with the main section, and the characteristics of these two sections were different. A plane problem for a five-section beam floating on the surface of a finite-depth fluid was considered in [2]. All sections were identical and connected by simple hinges. For the case of scattering of incoming surface waves by such a beam, the maximum amplitudes of deflections were demonstrated to occur at the points of the hinged joint. The behavior of a five-section rectangular plate exposed to head surface waves was studied in [3]. The elasticity parameters and the size of the sections at which the hinged joint produced a substantial effect were estimated. The solution for a two-section beam floating on the surface of a finite-depth fluid was given in [4, 5] for a beam with identical sections [4] and for a beam with sections of different lengths and different structural characteristics [5]. The behavior of an elongated two-section rectangular plate with oblique incidence of surface waves was considered in [6]. It was demonstrated that the elasticity of the hinged joint and the properties of individual sections exerted a significant effect on the hydroelastic behavior of the compound plate.

Lavrent'ev Institute of Hydrodynamics, Siberian Division, Russian Academy of Sciences, Novosibirsk 630090; sturova@hydro.nsc.ru. Translated from Prikladnaya Mekhanika i Tekhnicheskaya Fizika, Vol. 50, No. 4, pp. 54–65, July–August, 2009. Original article submitted February 19, 2008; revision submitted June 11, 2008.

In the present paper, we propose a method of solving a linear unsteady problem of the behavior of a floating two-section elastic beam plate. The following cases are considered as examples of the unsteady behavior: incidence of a localized surface wave onto the plate and initial deformation of the plate. These cases were studied for a homogeneous plate floating on shallow water in [7] and under the action of an arbitrary external load in [8].

1. Formulation of the Problem. Let an elastic beam of length $2L$ consisting of two sections connected by a simple hinge float freely on the surface of an ideal incompressible fluid layer of depth H. The structural characteristics of both sections of the beam are identical. The fluid surface that is not covered by the beam is considered as a free surface. The domain S occupied by the fluid is divided into three parts: S_1 ($|x| < L$), S_2 ($x < -L$), and S_3 ($x > L$) (x is the horizontal coordinate). The fluid depth is assumed to be small as compared with the length of the surface and flexural-gravity waves, and the shallow water approximation is used. The velocity potentials that describe the fluid motion in the domains S_j are $\varphi_j(x,t)$ ($j = 1, 2, 3$), where t is the time.

Let a localized surface wave be incident onto the beam from the left. The vertical displacement of the fluid in this wave is $\eta_0(x,t) = f(x - \sqrt{gH}\,t)$. The function $f(\xi)$ differs from zero only at $|\xi| < c$. Such a wave can arise as a result of the collapse of the initial elevation of the free surface at the time $t = t_0$ under the condition that the entire fluid is at rest at the initial time. In this case, the free surface at $t > t_0$ is known to consist of two localized waves moving without deformation in the opposite directions with a velocity $\sqrt{gH}$ [9]. The amplitudes of these waves are equal to one half of the amplitude of the initial elevation, and the width of the region occupied by each wave is equal to the width of the initial elevation region. It is assumed that the beam and the fluid at the time $t = 0$ are at rest in the domains S_1 and S_3, while the localized disturbance reaches the left edge of the beam in the domain S_2. At $t > 0$, the beam and the fluid start to oscillate in the domain S_1, which induces wave disturbances expanding from the plate in the domains S_2 and S_3.

The normal deflection of the Euler beam $w(x,t)$ is described by the equation

$$D\,\frac{\partial^4 w}{\partial x^4} + m\,\frac{\partial^2 w}{\partial t^2} + g\rho w + \rho\,\frac{\partial \varphi_1}{\partial t} = 0 \qquad (x \in S_1), \tag{1.1}$$

where D is the coefficient of cylindrical stiffness of both sections of the beam, m is their specific mass, ρ is the density of water, and g is the acceleration due to gravity.

According to the linear shallow water theory, the following relation is valid:

$$\frac{\partial w}{\partial t} = -h\,\frac{\partial^2 \varphi_1}{\partial x^2} \quad (x \in S_1), \qquad h = H - d \tag{1.2}$$

($d = m/\rho$ is the beam draft).

The velocity potentials outside the beam satisfy the equations

$$\frac{\partial^2 \varphi_j}{\partial t^2} = gH\,\frac{\partial^2 \varphi_j}{\partial x^2} \quad (x \in S_j), \qquad j = 2, 3. \tag{1.3}$$

The elevations of the free surface $\eta_2(x,t)$ and $\eta_3(x,t)$ in the domains S_2 and S_3 are found from the relations

$$\eta_j = -\frac{1}{g}\,\frac{\partial \varphi_j}{\partial t} \quad (x \in S_j), \qquad j = 2, 3.$$

The free hinge is assumed to be located at the point $x = x_1$ ($|x_1| < L$). The following notations are introduced:

$$w(x,t) = \begin{cases} w^-(x,t), & -L \leqslant x < x_1, \\ w^+(x,t), & x_1 < x \leqslant L. \end{cases}$$

The following conditions are satisfied at the hinge point (see, e.g., [1] for more details):

$$w^- = w^+, \qquad \frac{\partial^2 w^-}{\partial x^2} = \frac{\partial^2 w^+}{\partial x^2} = 0, \qquad \frac{\partial^3 w^-}{\partial x^3} = \frac{\partial^3 w^+}{\partial x^3} \qquad (x = x_1).$$

The free-edge conditions (zero bending moment and shear force) are imposed on the beam edges:

$$\frac{\partial^2 w^-}{\partial x^2} = \frac{\partial^3 w^-}{\partial x^3} = 0 \quad (x = -L), \qquad \frac{\partial^2 w^+}{\partial x^2} = \frac{\partial^3 w^+}{\partial x^3} = 0 \quad (x = L).$$

The conditions of continuity of pressure and mass have to be satisfied in the fluid at $x = \pm L$:

$$\frac{\partial \varphi_1}{\partial t} = \frac{\partial \varphi_2}{\partial t}, \qquad \frac{\partial \varphi_1}{\partial x} = \frac{H}{h}\,\frac{\partial \varphi_2}{\partial x} \qquad (x = -L); \qquad \frac{\partial \varphi_1}{\partial t} = \frac{\partial \varphi_3}{\partial t}, \qquad \frac{\partial \varphi_1}{\partial x} = \frac{H}{h}\,\frac{\partial \varphi_3}{\partial x} \qquad (x = L). \tag{1.4}$$

The conditions of the absence of disturbances are imposed far from the beam:

$$\frac{\partial \varphi_2}{\partial x} \to 0 \quad (x \to -\infty), \qquad \frac{\partial \varphi_3}{\partial x} \to 0 \quad (x \to \infty).$$

The initial conditions have the form

$$w = \eta_3 = \frac{\partial \varphi_1}{\partial t} = \frac{\partial \varphi_3}{\partial t} = 0, \qquad \eta_2 = \eta_0, \qquad \frac{\partial \varphi_2}{\partial t} = -g\eta_0 \qquad (t = 0). \tag{1.5}$$

Let us pass to dimensionless variables, using L as the length scale and $\sqrt{L/g}$ as the time scale.

The following dimensionless coefficients are used in what follows:

$$\delta = D/(\rho g L^4), \qquad \gamma = d/L.$$

2. Method of Normal Modes. We seek for beam deflection in the form of an expansion with respect to eigenfunctions of oscillations of the compound beam with free edges in vacuum:

$$w(x,t) = \sum_{n=0}^{\infty} X_n(t) W_n(x). \tag{2.1}$$

Here, the functions $X_n(t)$ have to be determined, and the functions $W_n(x)$ are solutions of the following spectral problem in dimensionless variables:

$$W_n^{(\mathrm{IV})} = \lambda_n^4 W_n \qquad (|x| \leqslant 1),$$

$$(W_n^-)'' = (W_n^-)''' = 0 \quad (x = -1), \qquad (W_n^+)'' = (W_n^+)''' = 0 \quad (x = 1), \tag{2.2}$$

$$W_n^- = W_n^+, \qquad (W_n^-)'' = (W_n^+)'' = 0, \qquad (W_n^-)''' = (W_n^+)''' \qquad (x = x_1)$$

(the prime denotes differentiation with respect to x). These solutions have the form

$$W_0 = 1/\sqrt{2}, \qquad W_1 = \sqrt{3/2}\, x,$$

$$W_2^- = \sqrt{\frac{3(1 - x_1)}{2(1 + x_1)^3}}\, [1 + (2 + x_1)x], \qquad W_2^+ = \sqrt{\frac{3(1 + x_1)}{2(1 - x_1)^3}}\, [1 + (x_1 - 2)x],$$

$$W_n^- = B_n\{\sin(\lambda_n(x+1)) + \sinh(\lambda_n(x+1)) - D_n[\cos(\lambda_n(x+1)) + \cosh(\lambda_n(x+1))]\},$$

$$W_n^+ = B_n C_n\{\sin(\lambda_n(1-x)) + \sinh(\lambda_n(1-x)) - F_n[\cos(\lambda_n(1-x)) + \cosh(\lambda_n(1-x))]\},$$

where

$$D_n = \frac{\sin z_n - \sinh z_n}{\cos z_n - \cosh z_n}, \quad F_n = \frac{\sin v_n - \sinh v_n}{\cos v_n - \cosh v_n}, \quad C_n = \frac{(\cos v_n - \cosh v_n)(\sinh z_n \cos z_n - \cosh z_n \sin z_n)}{(\cos z_n - \cosh z_n)(\sinh v_n \cos v_n - \cosh v_n \sin v_n)},$$

$$B_n = \sqrt{\lambda_n/(z_n D_n^2 + v_n F_n^2 C_n^2)}, \qquad z_n = \lambda_n(1 + x_1), \qquad v_n = \lambda_n(1 - x_1). \tag{2.3}$$

The eigenvalues λ_n are determined from the equation

$$(\sinh z_n \cos z_n - \cosh z_n \sin z_n)(1 - \cosh v_n \cos v_n) + (\sinh v_n \cos v_n - \cosh v_n \sin v_n)(1 - \cosh z_n \cos z_n) = 0 \quad (n \geqslant 3),$$

$$\lambda_0 = \lambda_1 = \lambda_2 = 0. \tag{2.4}$$

In the space $L^2(-1,1)$, the functions $W_n(x)$ form a full orthogonal system normalized as follows:

$$\int_{-1}^{1} W_n(x) W_m(x)\, dx = \delta_{nm}$$

(δ_{nm} is the Kronecker delta).

If the hinged joint is located in the middle of the beam ($x_1 = 0$), then the system of eigenfunctions $W_n(x)$ decomposes into even and odd components with respect to x. For $k \geqslant 1$, the functions $W_{2k+1}(x)$ coincide with odd eigenfunctions for a homogeneous beam (see, e.g., [8]):

$$W_{2k+1}(x) = \frac{\sin(\lambda_{2k+1}x) + S_{2k+1}\sinh(\lambda_{2k+1}x)}{\sqrt{1 - S_{2k+1}^2}}, \qquad S_{2k+1} = \frac{\cos\lambda_{2k+1}}{\cosh\lambda_{2k+1}}.$$

The eigenvalues λ_{2k+1} are determined from the equation $\tan\lambda_{2k+1} = \tanh\lambda_{2k+1}$. For $k \geqslant 2$, the functions $W_{2k}(x)$ have the form

$$W_{2k}(x) = B_{2k}\{\sin(\lambda_{2k}(1 - |x|)) + \sinh(\lambda_{2k}(1 - |x|)) - D_{2k}[\cos(\lambda_{2k}(1 - |x|)) + \cosh(\lambda_{2k}(1 - |x|))]\},$$

where the values of B_{2k} and D_{2k} are determined from Eqs. (2.3) with $z_{2k} = v_{2k} = \lambda_{2k}$. The eigenvalues λ_{2k} satisfy the equation $\cos\lambda_{2k}\cosh\lambda_{2k} = 1$.

Substituting expansions (2.1) into Eqs. (1.1) and the initial conditions (1.5), multiplying the resultant relations by $W_m(x)$, and integrating them with respect to x from -1 to 1, we obtain the system of ordinary differential equations (ODE)

$$\gamma\ddot{X}_m + (\delta\lambda_m^4 + 1)X_m + f_m(t) = 0, \qquad X_m(0) = \dot{X}_m(0) = 0,$$

where

$$f_m(t) = \int_{-1}^{1} W_m \frac{\partial\varphi_1}{\partial t}\,dx,$$

and the over-dot indicates differentiation with respect to time.

The solution for $\varphi_1(x,t)$ is sought in the form

$$\varphi_1(x,t) = -\frac{1}{h}\Big[V(t) + xU(t) + \sum_{k=1}^{\infty} Q_k(t)\sin\Big(\frac{k\pi}{2}(x+1)\Big)\Big]. \tag{2.5}$$

Substituting this expansion into Eq. (1.2), multiplying the resultant relation by $\sin[m\pi(x+1)/2]$, and integrating it with respect to x from -1 to 1, we obtain

$$Q_m(t) = -\frac{4}{\pi^2 m^2}\sum_{n=0}^{\infty}\dot{X}_n(t)P_{nm},$$

where

$$P_{nm} = \int_{-1}^{1} W_n(x)\sin\Big(\frac{m\pi}{2}(x+1)\Big)\,dx.$$

The values of P_{nm} are calculated analytically, but the expressions for these quantities are not given here, being too cumbersome. The functions $V(t)$ and $U(t)$ are determined from the matching conditions (1.4).

Let us consider the behavior of the solution in the domains S_2 and S_3. The solution for $\varphi_2(x,t)$ is sought in the form

$$\varphi_2(x,t) = \varphi_0(x,t) + \psi(x,t),$$

where $\varphi_0(x,t)$ is the potential of the incident wave, which is found from the relation

$$\frac{\partial\varphi_0}{\partial x} = \frac{\eta_0}{\sqrt{H}}.$$

The function $\psi(x,t)$ describes the velocity potential of the reflected wave. According to Eq. (1.3), the solution for $\psi(x,t)$ can be sought in the form

$$\psi(x,t) = \begin{cases} A((x+1)/\sqrt{H} + t), & -(1 + \sqrt{H}\,t) < x < -1, \\ 0, & x < -(1 + \sqrt{H}t). \end{cases} \tag{2.6}$$

A similar presentation is obtained for the function $\varphi_3(x,t)$, which describes the velocity potential of the transmitted wave:

$$\varphi_3(x,t) = \begin{cases} B(t - (x-1)/\sqrt{H}\,), & 1 < x < 1 + \sqrt{H}t, \\ 0, & x > 1 + \sqrt{H}\,t. \end{cases} \tag{2.7}$$

The functions $A(\xi)$ and $B(\xi)$ in formulas (2.6) and (2.7) are unknown. Using the matching conditions (1.4), we obtain the differential equations for these functions in the form

$$\dot{A} = \frac{1}{\sqrt{H}}\Big(\frac{2}{\pi}\sum_{n=0}^{\infty}\dot{X}_n R_n - U\Big) - \alpha(t), \qquad \dot{B} = \frac{1}{\sqrt{H}}\Big(U - \frac{2}{\pi}\sum_{n=0}^{\infty}\dot{X}_n Z_n\Big) \tag{2.8}$$

with the initial conditions $A(0) = B(0) = 0$, where

$$\alpha(t) = \eta_0(-1,t), \qquad R_n = \sum_{k=1}^{\infty}\frac{P_{nk}}{k}, \qquad Z_n = \sum_{k=1}^{\infty}(-1)^k\,\frac{P_{nk}}{k}.$$

Using the relations obtained, we write the final ODE system for determining beam oscillations in the form

$$\sum_{n=0}^{\infty}\Big(\gamma\delta_{nm} + \frac{4}{\pi^2 h}\,T_{nm}\Big)\ddot{X}_n + (\delta\lambda_m^4 + 1)X_m - \sqrt{2}\,\Big(\alpha(t) + \frac{1}{\pi\sqrt{H}}\sum_{n=0}^{\infty}(Z_n - R_n)\dot{X}_n\Big)\delta_{0m}$$

$$+\sqrt{\frac{2}{3}}\,\Big[\alpha(t) + \frac{1}{\sqrt{H}}\Big(U - \frac{1}{\pi}\sum_{n=0}^{\infty}(Z_n + R_n)\dot{X}_n\Big)\Big]\delta_{m1} = 0, \tag{2.9}$$

$$\dot{U} = -h\Big[\alpha(t) + \frac{1}{\sqrt{H}}\Big(U - \frac{1}{\pi}\sum_{n=0}^{\infty}(Z_n + R_n)\dot{X}_n\Big)\Big],$$

where

$$T_{mn} = \sum_{k=1}^{\infty}\frac{P_{nk}P_{mk}}{k^2}.$$

Determining the functions $X_n(t)$ and $U(t)$, we can find all characteristics of motion of the fluid and the elastic beam. For instance, the vertical elevations of the free surface in the domain S_2 are

$$\eta_2(x,t) = \eta_0(x,t) + \zeta(x,t),$$

$$\zeta(x,t) = \begin{cases} -\dot{A}((x+1)/\sqrt{H} + t), & -(1+\sqrt{H}t) < x < -1, \\ 0, & x < -(1+\sqrt{H}\,t), \end{cases}$$

and these elevations in the domain S_3 are

$$\eta_3(x,t) = \begin{cases} -\dot{B}(t - (x-1)/\sqrt{H}\,), & 1 < x < 1 + \sqrt{H}\,t, \\ 0, & x > 1 + \sqrt{H}\,t \end{cases}$$

[the functions $\dot{A}(\xi)$ and $\dot{B}(\xi)$ are determined in Eq. (2.8)].

3. Energy Relation. Let us determine the time evolution of the energies of the transmitted and reflected waves. The total energy of the incident wave is [9]

$$E_0 = \int\limits_{-(1+2c)}^{-1}\eta_0^2(x,0)\,dx.$$

This energy is transferred to oscillations of the elastic plate and scattered (transmitted and reflected) surface waves. As $t \to \infty$, plate oscillations decay, and the plate returns to the initial horizontal location. The energy of the reflected wave is

$$E_r(t) = \int\limits_{-(1+\sqrt{H}t)}^{-1}\zeta^2(x,t)\,dx = \sqrt{H}\int\limits_0^t \dot{A}^2(\xi)\,d\xi,$$

and the energy of the transmitted wave is

$$E_t(t) = \int\limits_{1}^{1+\sqrt{H}\,t}\eta_3^2(x,t)\,dx = \sqrt{H}\int\limits_0^t \dot{B}^2(\xi)\,d\xi.$$

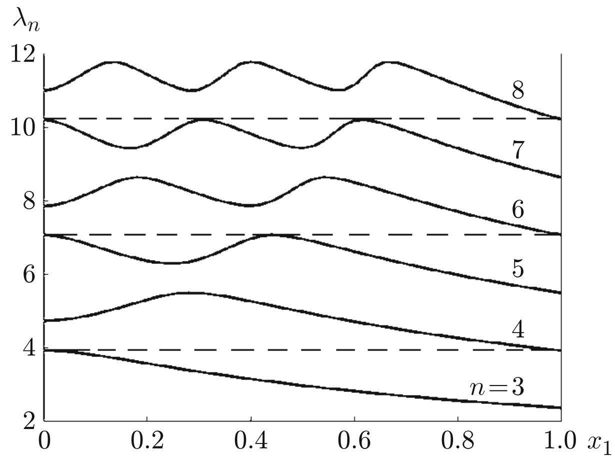

Fig. 1. Eigenvalues λ_n ($n = 3, \ldots, 8$) versus the hinge coordinate x_1: the dashed curves are the eigenvalues for antisymmetric modes of a homogeneous beam.

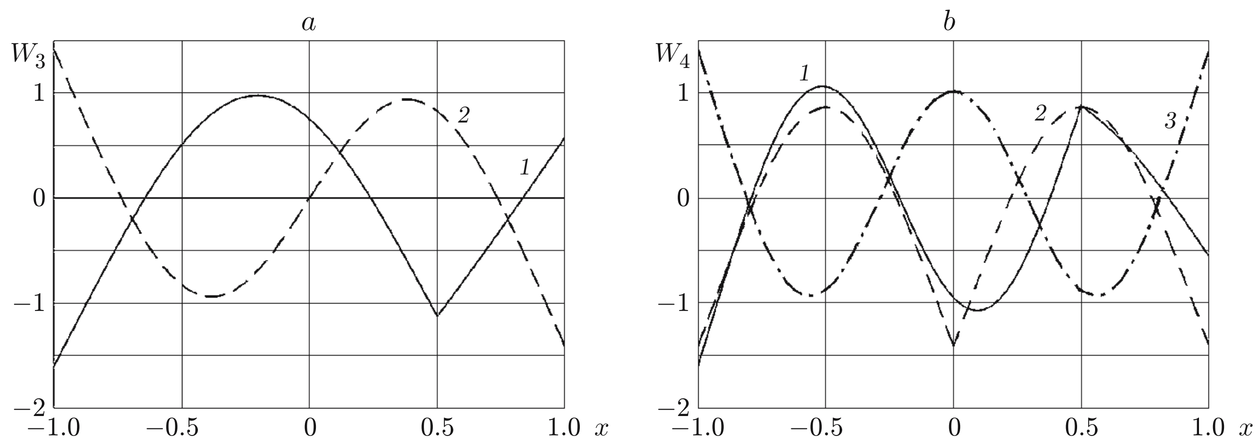

Fig. 2. Eigenfunctions $W_3(x)$ (a) and $W_4(x)$ (b): curves 1 and 2 refer to a compound beam with $x_1/L = 0.5$ (1) and $x_1 = 0$ (2); curve 3 refers to a homogeneous beam.

This problem does not involve energy dissipation; hence, we obtain

$$\lim_{t\to\infty} E(t) = E_0, \qquad E(t) = E_r(t) + E_t(t).$$

Satisfaction of this equality can serve as a criterion of accuracy of the method used.

4. Calculation Results. Using the reduction method, we replace the infinite series in expansions (2.1), (2.5) by sums with the number of terms N and K, respectively. The ODE system (2.9) is solved numerically by the fourth-order Runge–Kutta method.

Figure 1 shows the eigenvalues λ_n determined by solving Eq. (2.4) for modes with numbers $n = 3, \ldots, 8$ as functions of the hinge coordinate x_1. As $x_1 \to 1$, the eigenvalues correspond to a homogeneous beam. At $x_1 = 0$, the eigenvalues with odd numbers λ_{2k+1} at $k \geqslant 1$ coincide with the eigenvalues for antisymmetric modes of a homogeneous beam (dashed curves in Fig. 1). Note that there are only two eigenfunctions for a homogeneous beam at a zero eigenvalue (the so-called rigid-body modes (see, e.g., [8])). Addition of each next hinge increases the multiplicity of the zero eigenvalue and, correspondingly, the number of eigenfunctions. For a five-section beam, for instance, there are six eigenfunctions at the zero eigenvalue [3].

Figure 2 shows the eigenfunctions $W_n(x)$ ($n = 3, 4$). As was noted above, antisymmetric eigenfunctions at $x_1 = 0$ coincide with the corresponding eigenfunctions for a homogeneous beam. At $x_1 = 0.5$, the eigenvalues are $\lambda_3 = 2.9745$ and $\lambda_4 = 4.9772$; at $x_1 = 0$, the eigenvalues are $\lambda_3 = 3.9266$ and $\lambda_4 = 4.7300$; for a homogeneous beam, $\lambda_4 = 5.4978$. If there is a hinge, the functions $W_n(x)$ have inflections at the point $x = x_1$, and the maximum absolute values of these functions can occur both at the beam edges and at the hinge point.

The following dimensional initial parameters are used in the calculations: $L = 500$ m, $d = 5$ m, $\delta = 5 \cdot 10^{-3}$, $\rho = 10^3$ kg/m^3, and $H = 20$ m. In all calculations performed, the number of beam oscillation modes is $N = 25$, the number of harmonics in Eq. (2.5) is $K = 200$, and a further increase in the values of N and K has almost no effect on the result.

The shape of the localized surface wave incident onto the elastic beam is chosen as

$$f(\xi) = \begin{cases} (a/2)(1 + \cos(\pi\xi/c)), & |\xi| < c, \\ 0, & |\xi| > c, \end{cases}$$

where $\xi = x - t\sqrt{gH} - x_0$. The total energy of such a wave is constant in time and equal to

$$E_0 = \rho g \int_{-c}^{c} f^2(\xi)\, d\xi = \frac{3}{4}\, \rho g a^2 c.$$

Figure 3 shows the shapes of the free surface and the beam at $x_0/L = -1.25$ and $c/L = 0.25$ at the time $t\sqrt{g/L} = 10$. This time corresponds to the moment when the initial wave passes under the beam, which results in beam deformation. Obviously, beam deflections and the shape of the free surface depend essentially on the presence and location of the hinged joint.

The dimensionless values of the coefficients $X_0, X_1, \ldots, X_7$ and the function u at $t\sqrt{g/L} = 10$ for four variants of the beam shown in Fig. 3 are summarized in Table 1. The coefficients X_0 and X_1 corresponding to the so-called rigid-body modes are seen to have the highest values. The absolute values of the function u are close to the values of the coefficient X_3. It follows from Table 1 that the absolute values of X_n decrease rather rapidly with increasing n.

Figure 4 shows the time evolution of the total energy of the transmitted and reflected waves E and the total energy of the reflected wave E_r for four variants of the beam. It is seen that the highest value of the total energy for all variants of the beam considered is reached at $t\sqrt{g/L} \approx 15$. By this time, beam oscillations cease, and a considerable portion of the initial energy of the incident wave is transformed to the energy of the transmitted wave. The most intense scattering of energy in the reflected wave occurs at $x_1/L = \pm 0.5$ and amounts approximately to 25% of the initial energy, while this value for a homogeneous beam is approximately 10%. The intermediate value of reflected wave energy (equal approximately to 15%) is observed at $x_1 = 0$. Therefore, the presence of a hinged joint can exert a significant effect on transformation of the incident wave.

Let us also consider the unsteady behavior of the beam with its initial deformation in a quiescent fluid. The initial conditions for this problem have the form

$$w(x, 0) = w_0(x), \qquad \frac{\partial w}{\partial t}\Big|_{t=0} = 0,$$

$$\varphi_j(x, 0) = 0 \quad (j = 1, 2, 3), \qquad \eta_2(x, 0) = \eta_3(x, 0) = 0.$$

The function $w_0(x)$ is chosen in the form

$$w_0(x) = (a/2)(1 + \cos(\pi x/L)).$$

In this problem, there is no external loading, and the ODE system for determining beam oscillations coincides with system (2.9) under the condition $\alpha(t) \equiv 0$. The initial conditions for $X_m(0)$ are given by the relations

$$X_m(0) = \int_{-1}^{1} w_0(x) W_m(x)\, dx, \qquad \dot{X}_m(0) = 0.$$

Figure 5 shows the normal deflection of the beam as a function of time. It is seen that the effect of the hinged joint is essential only at the initial time instants, and the deflections of a compound beam are more pronounced than the deflections of a homogeneous beam (Figs. 5b–5d). Beam oscillations decay with time, and the presence of the hinge almost ceases to exert any noticeable effect (Fig. 5f).

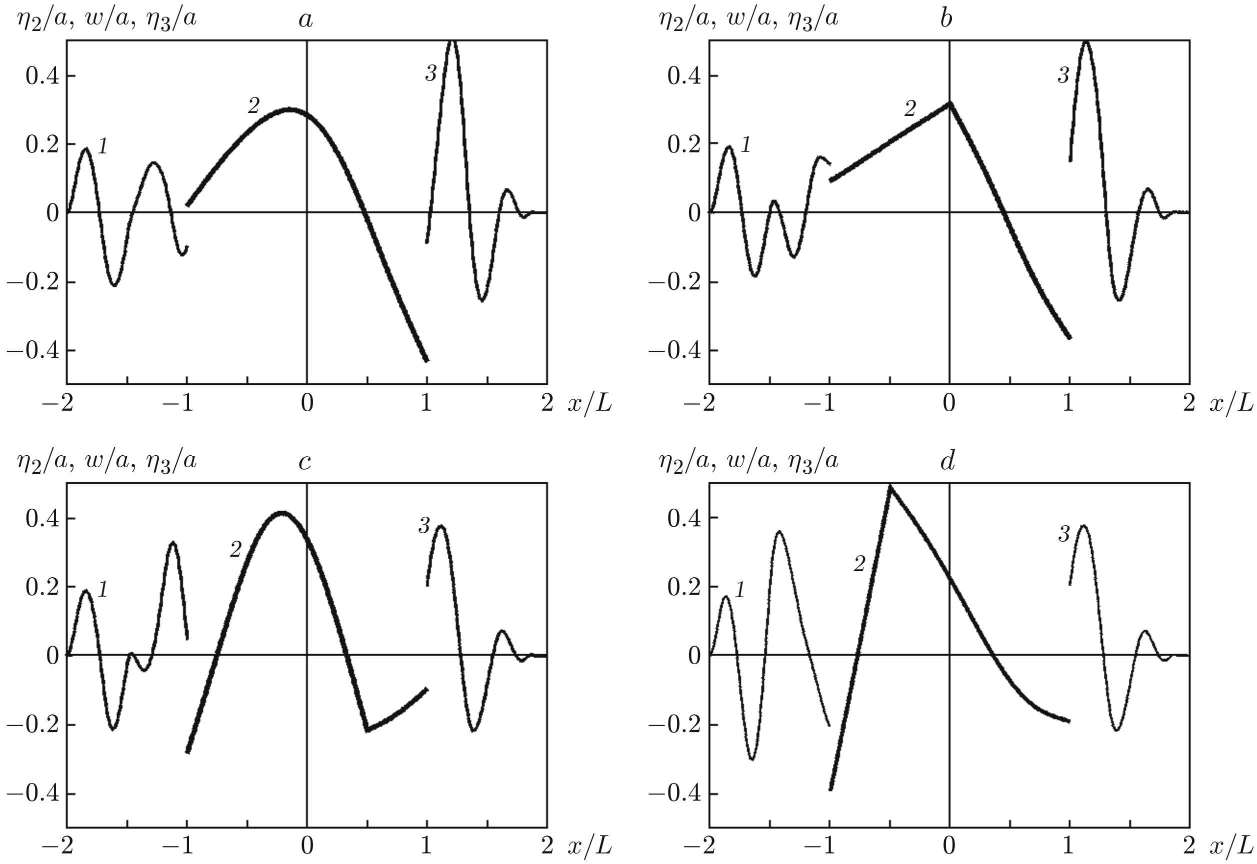

Fig. 3. Shapes of the free surface and the beam at $t\sqrt{g/L} = 10$ for a homogeneous beam (a) and a compound beam with $x_1 = 0$ (b), $x_1/L = 0.5$ (c), and $x_1/L = -0.5$ (d); the curves show the behavior of η_2/a (1), w/a (2), and η_3/a (3).

TABLE 1

Dimensional Values of the Coefficients $X_0, X_1, \ldots, X_7$ and Function u at $t\sqrt{g/L} = 10$ for Four Variants of the Beam

Coefficient	Homogeneous beam	Compound beam		
		$x_1 = 0$	$x_1/L = 0.5$	$x_1/L = -0.5$
X_0	0.16428	0.17929	0.15591	0.17270
X_1	0.14578	0.14635	0.20638	0.17565
X_2	−0.05050	−0.04562	−0.01729	−0.05348
X_3	0.01949	0.02007	−0.02095	0.02931
X_4	−0.00309	0.01153	0.00014	0.01175
X_5	0.00023	0.00023	−0.00272	−0.00098
X_6	0.00011	0.00043	−0.00004	0.00001
X_7	−0.00001	−0.00001	−0.00031	−0.00005
u	−0.01583	−0.01883	−0.02262	−0.02083

In this problem, it is also of interest to study the behavior of the eigenvalues of the ODE system (2.9), which can be written after reduction in the matrix form as

$$\dot{\boldsymbol{Y}} = C\boldsymbol{Y} + \boldsymbol{F}(t),$$

where $\boldsymbol{Y} = \{X_0, X_1, \ldots, X_{N-1}; \dot{X}_0, \dot{X}_1, \ldots, \dot{X}_{N-1}; U\}^{\mathrm{t}}$; C is a square matrix of the order $2N+1$ with constant elements; the vector $\boldsymbol{F}(t)$ is defined by unsteady loading.

The eigenvalues and eigenvectors of the matrix C are often called "wet" modes, in contrast to the eigenvalues and eigenfunctions of problem (2.2), which are called "dry" modes. The properties of "dry" modes are determined

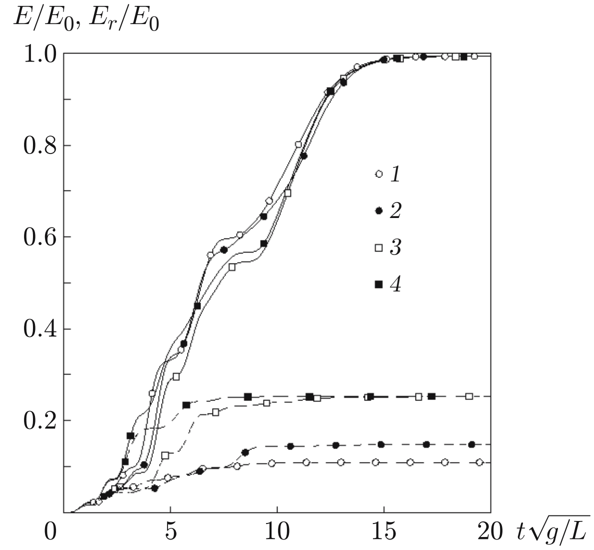

Fig. 4. Time evolution of the total energy E/E_0 (solid curves) and reflected wave energy E_r/E_0 (dashed curves) for a homogeneous beam (1) and for a compound beam with $x_1 = 0$ (2), $x_1/L = 0.5$ (3), and $x_1/L = -0.5$ (4).

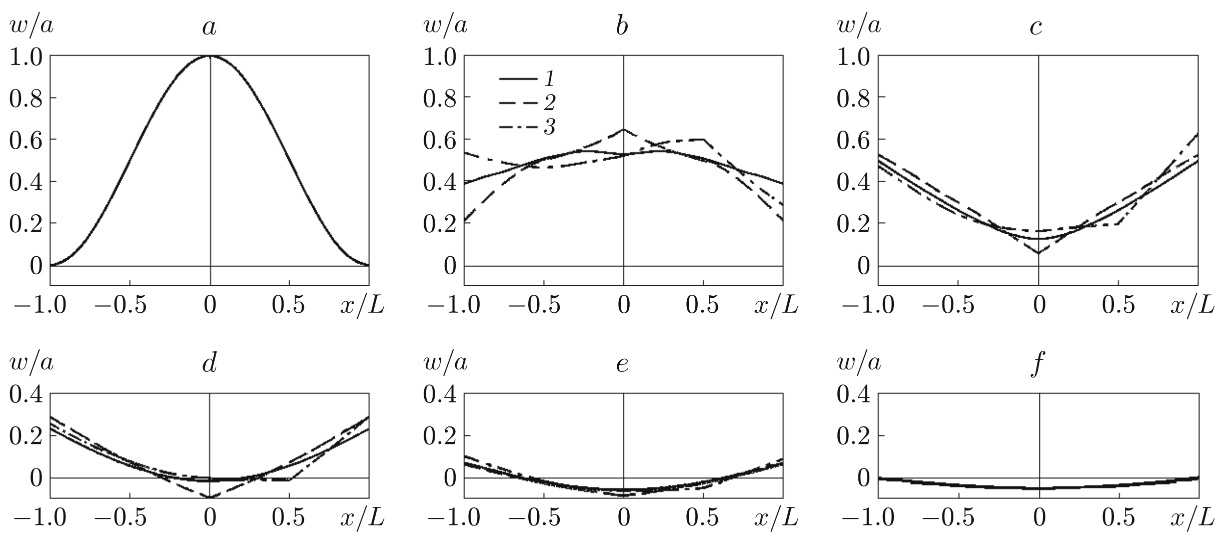

Fig. 5. Beam deformation caused by its initial deformation: $t\sqrt{g/L} = 0$ (a), 2.5 (b), 5 (c), 7.5 (d), 10 (e), and 12.5 (f); curve 1 refers to a homogeneous beam; curves 2 and 3 refer to a compound beam with $x_1 = 0$ (2) and $x_1/L = 0.5$ (3).

only by the structural features of the beam, while the properties of "wet" modes depend also on the fluid properties but do not depend on the type of unsteady loading.

The eigenvalues of the matrix C are determined numerically. This matrix has one purely real eigenvalue μ_0 and $2N$ complex-conjugate eigenvalues μ_k ($k = \pm 1, \pm 2, \ldots, \pm N$). The real parts of all eigenvalues are negative. Let us enumerate the eigenvalues in the order of increasing imaginary part: $\operatorname{Im} \mu_k < \operatorname{Im} \mu_{k+1}$. The sign of the number k corresponds to the sign of the imaginary part of the eigenvalue.

Figure 6 shows the real and imaginary parts of the eigenvalues μ_k ($k = 0, 1, 2, 3$) as functions of the hinge coordinate. It is seen that the effect of the value of x_1 on the lower "wet" modes is rather weak. This may be responsible for the fact that the effect of the hinge in the case of free oscillations of the beam induced by its initial disturbance is rather pronounced only at small times, when the higher modes make noticeable contributions. The influence of these modes becomes weaker with time, because they decay faster than lower modes.

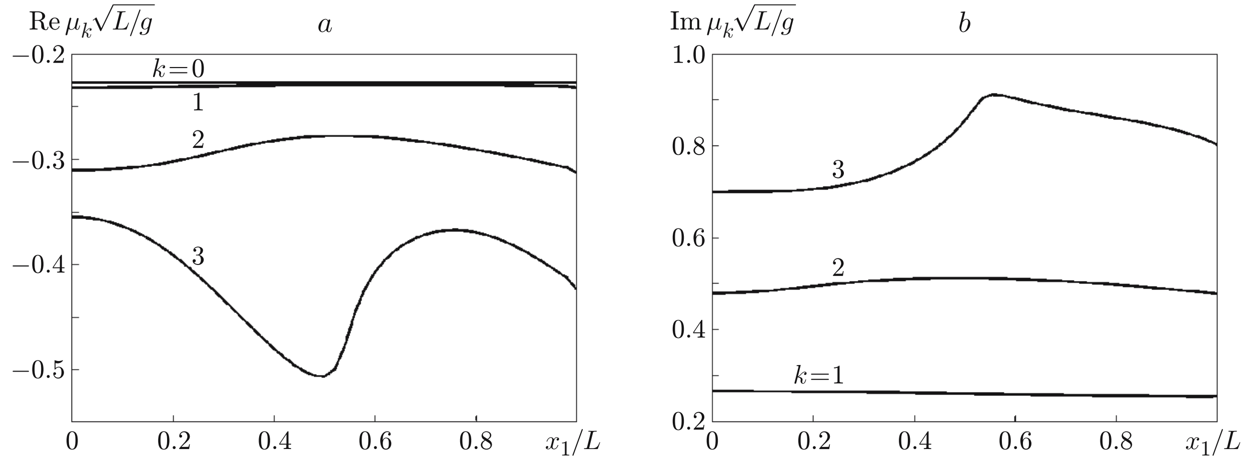

Fig. 6. Real part (a) and imaginary part (b) of the eigenvalues μ_k of the matrix C versus the hinge coordinate for modes with numbers $k = 0$, 1, 2, and 3.

With the use of the results obtained in [10], the proposed method of solving an unsteady problem can be extended to the case of a compound beam floating on the surface of an infinitely deep fluid.

This work was supported by the Russian Foundation for Basic Research (Grant No. 07-08-00145) and by the Integration Project No. 2.12 of the Siberian Division of the Russian Academy of Sciences.

REFERENCES

1. I. V. Sturova, "Diffraction of surface waves on an inhomogeneous elastic plate," *J. Appl. Mech. Tech. Phys.*, **41**, No. 4, 612–618 (2000).
2. D. Xia, J. W. Kim, and R. C. Ertekin, "On the hydroelastic behavior of two-dimensional articulated plates," *Marine Structures*, **13**, Nos. 4/5, 261–278 (2000).
3. J. N. Newman, "Efficient hydrodynamic analysis of very large floating structures," *Marine Structures*, **18**, No. 2, 169–180 (2005).
4. D. Karmakar and T. Sahoo, "Scattering of waves by articulated floating elastic plates in water of infinite depth," *Marine Structures*, **18**, Nos. 5/6, 451–471 (2005).
5. T. I. Khabakhpasheva and A. A. Korobkin, "Hydroelastic behaviour of compound floating plate in waves," *J. Eng. Math.*, **44**, No. 1, 21–40 (2002).
6. S. Fu, T. Moan, X. Chen, and W. Cui, "Hydroelastic analysis of flexible floating structures with rigid-hinge-mode," in: *Proc. of the 4th Int. Conf. on Hydroelasticity in Marine Technology* (Wuxi, China, September 10–14, 2006), Nat. Defense Industry Press, Beijing (2006), pp. 235–244.
7. M. H. Meylan, "Spectral solution of time-dependent shallow water hydroelasticity," *J. Fluid Mech.*, **454**, 387–402 (2002).
8. I. V. Sturova, "Unsteady behavior of an elastic beam floating on shallow water under external loading," *J. Appl. Mech. Tech. Phys.*, **43**, No. 3, 415–423 (2002).
9. L. V. Cherkesov, V. A. Ivanov, and S. M. Khartiev, *Introduction into Hydrodynamics and Wave Theory* [in Russian], Gidrometeoizdat, St. Petersburg (1992).
10. I. V. Sturova, "Unsteady behavior of an elastic beam floating on the surface of an infinitely deep fluid," *J. Appl. Mech. Tech. Phys.*, **47**, No. 1, 71–78 (2006).